Reconstructing age and reactivity distributions from the moments carried by central-moment transport models

Shahram Asgari

Department of Marine Sciences, University of Georgia, Athens, GA 30602, USA

Email: shahram.asgari@uga.edu

ORCID: 0009-0004-3810-2739

This is a non-peer-reviewed preprint submitted to EarthArXiv. It has not undergone peer review. The manuscript is intended for submission to the peer-reviewed journal Transport in Porous Media.

Reconstructing age and reactivity distributions from the moments carried by central-moment transport models

Shahram Asgari

Department of Marine Sciences, University of Georgia, Athens, GA 30602, USA

Correspondence: shahram.asgari@uga.edu

ORCID: https://orcid.org/0009-0004-3810-2739

Abstract

A central-moment transport model follows a property that varies across a population, such as the age of water parcels or the decay rate of organic-matter particles. Instead of storing the whole distribution of that property, it keeps only a few summary numbers, the moments, and moves those through the model. But the distribution itself is usually what a scientist wants, so it has to be rebuilt from the moments afterward. This rebuilding is an old problem, because many different distributions share the same few moments. It is well understood in aerosol and population-balance modeling, but it has not been tested for age and reactivity distributions. Here we bring those methods to the age and reactivity setting and measure how well they work against fully resolved references. We test five ways to rebuild a distribution from its moments, the gamma, log-normal, translated Weibull, and maximum-entropy shapes and a triangle, and we score each by the area between the rebuilt curve and the true one. The result is simple. Accuracy depends on how well the assumed shape matches the true shape, not on how many moments are carried. The log-normal shape wins on a log-normal reference, with an error of 0.03 against 0.04 for the gamma; the gamma wins on a gamma reference at 0.02; and the three-moment Weibull wins on the skewed age distribution at 0.06, while the triangle cannot fit these skewed shapes at all. The error grows as pore-scale mixing increases. Storing the maximum-entropy shape in a lookup table makes it about 700 times faster to use, but the gamma and Weibull shapes are already far cheaper, so the table helps only when maximum entropy is needed.

Article Highlights

- The accuracy of a reconstructed age or reactivity distribution is set mainly by how well the assumed shape matches the true shape, not by the number of moments carried.
- The reconstruction error grows as pore-scale mixing increases, measured with a bounded, shape-based error and confirmed against a particle reference whose tail is not truncated.
- Precomputing the maximum-entropy fit as a lookup table speeds it up about 700-fold, but the recommended gamma and Weibull fits are already far cheaper.

Keywords Reactive transport, Residence time distribution, Method of moments, Moment reconstruction, Maximum entropy, Reactivity continuum

1. Introduction

Reactive-transport models increasingly describe a chemical species not by how much of it is present, but by how a property is spread across it. Two examples are common. One is the range of travel times among the water parcels in a sample. The other is the range of decay rates among the

particles of organic matter in a sediment (Ginn 1999; Boudreau and Ruddick 1991; Arndt et al. 2013). Following that full spread at every point in a model is expensive, because it takes many separate classes in every grid cell. To save that cost, central-moment models keep only the lowest few moments of the distribution, a handful of summary numbers such as the mean, the variance, and sometimes the skewness, and they move and react those numbers directly (Rooze et al. 2023).

A moment-transport model is, however, only half of a workflow. The output a scientist actually wants to read is usually the distribution itself, for example the shape of the travel-time distribution or the spread of reactivities, and that shape has to be rebuilt from the few moments the model carries. Rebuilding a density from a finite number of its moments is a classical and still-active problem. It has been studied for decades in aerosol science and population-balance modeling, under names such as the quadrature method of moments and its variants (McGraw 1997; Marchisio and Fox 2005) and the extended quadrature method of moments, which assembles a density from gamma, log-normal or Weibull building blocks (Yuan et al. 2012), as well as more general moment-reconstruction techniques (John et al. 2007). A related literature asks when the problem is even solvable: how hard the maximum-entropy version is to solve, and the limits on which sets of moments come from a real distribution at all, are treated by Mead and Papanicolaou (1984), Levermore (1996), Junk (1998) and Abramov (2010).

Rooze et al. (2023) raised the rebuilding step specifically for age and reactivity distributions. They reported that the error is largest in the tails of the distribution, noted that a triangular shape breaks down when the distribution is strongly skewed, and suggested that precomputed lookup tables could make a flexible shape affordable. Those observations were made in passing, and were not quantified against a resolved reference.

In the present study we test that rebuilding step directly. We first generate reference age and reactivity distributions in a one-dimensional column that holds two kinds of pore space, a fast-flowing mobile one where the water actually moves, and a stagnant immobile one where water is trapped and exchanges solute only by slow diffusion. For reactivity, we picture the organic matter as a mix of many compounds with different decay rates, from fast to slow. As this mix moves through the column, the fast-decaying compounds are consumed first, so what reaches the outlet is weighted toward the slower rates. The relative amount of each decay rate in the material leaving the column forms a curve, the reactivity distribution, and this is one reference we try to rebuild. For age, we release tracer particles and record how long each one takes to cross the column; the spread of these travel times forms a second curve, the age distribution. A moment model does not store such a curve. It keeps only two or three numbers that summarize it, its average value, its width, and sometimes its tilt to one side, and these numbers are its moments. The hard part is going backward: from those two or three numbers alone, we try to redraw the whole curve, testing five candidate shapes such as a gamma or a log-normal, and we measure how close each redrawn curve comes to the true one. On that basis we answer three questions with quantitative evidence. First, how much does the choice of shape matter, compared with the number of moments carried? Second, how does the reconstruction error change as the transport becomes more mixing-limited? Third, can the reconstruction be precomputed cheaply, and is that worth doing? Section 2 sets out the reference distributions, the reconstruction methods, and the error measures. Section 3 reports and discusses the results. Section 4 concludes.

2. Methods

The rest of this section follows the same steps as the introduction. Section 2.1 makes precise what a moment model stores and why rebuilding is hard. Section 2.2 builds the reference distributions, first the column, then the reactivity distribution and the age distribution. Section 2.3 gives the five methods we use to rebuild a distribution from its moments. Section 2.4 defines how we measure the error. Section 2.5 adds a lookup table that makes one method fast.

2.1. What a moment model stores, and why rebuilding is hard

The introduction gave the idea in words; here we make it precise. Write $g(\chi)$ for the distribution of the carried property χ, an age or a decay rate. This is the full curve. A moment model never carries $g(\chi)$ itself. It carries only a few numbers taken from that curve, its moments, defined as

$$C = \int g(\chi)\, d\chi\,, \tag{1}$$

$$\mu = (1/C) \int \chi\, g(\chi)\, d\chi\,, \tag{2}$$

$$\varphi_q = (1/C) \int (\chi - \mu)^q\, g(\chi)\, d\chi\,, \quad q \geq 2\,, \tag{3}$$

Here C is the total amount of the species (the zeroth moment); μ is the mean, the average value; and φ_q is the central moment of order q, so that φ_2 is the variance, the width, and φ_3 sets the skewness, the tilt to one side. These are the same average, width, and tilt described in the introduction. The model moves C, μ, and one or two φ_q down the column and reacts them in place. Rebuilding is the reverse step: from the short list $\{C, \mu, \varphi_2$, up to $\varphi_M\}$, find a curve $g(\chi)$ that matches those numbers. The trouble is that many curves share the same short list, so the numbers alone do not fix one curve; the problem is ill-posed. Each method must add something, either a fixed shape for the curve, or a rule that picks the smoothest curve still matching the numbers (the maximum-entropy method, below). In Sects. 3.1 to 3.4 we hand each method the exact moments of a known reference, found by direct numerical integration, so that we test the rebuilding step on its own. Section 3.5 then puts it inside a running model, where the moments are carried down the column and are only approximate.

2.2. Building the reference distributions

To measure reconstruction error we need reference distributions whose true shape we already know. We build them in a one-dimensional column with two pore spaces, a fast-flowing mobile space and a stagnant immobile space that trade solute with each other, following Rooze et al. (2023). The settings are a mobile porosity $\theta_m = 0.35$, an immobile porosity $\theta_{im} = 0.15$, a pore velocity $v = 1$, a dispersion coefficient $D = 0.01$, and a column length $L = 1$. Together they fix a Péclet number $vL/D = 100$; that is, advection is a hundred times stronger than diffusion. We hold this value fixed throughout. The mixing time τ_m sets how fast solute passes between the two pore spaces, through a first-order exchange coefficient $\omega = \theta_{im} / \tau_m$.

2.2.1. The reactivity distribution

For reactivity, the range of decay rates is split into 600 classes spanning $\chi \in [10^{-3}, 60]$. Each class i is carried to steady state through the column by a finite-volume solver on 201 cells, following

$$D\, d^2C_i/dx^2 - v\, dC_i/dx - s_i\, C_i = 0\,, \quad C_i(0) = 1\,, \quad dC_i/dx|_{x=L} = 0\,, \tag{4}$$

where $C_i(x)$ is the mobile concentration of class i along the column, and s_i is an effective loss rate that combines the decay of that class with the leakage of solute into the stagnant immobile pore,

$$s_i = \chi_i + (\omega/\theta_m)\,(\theta_{im}\,\chi_i)/(\omega + \theta_{im}\,\chi_i)\,, \tag{5}$$

with χ_i the decay rate of class i. The outlet distribution is then built from the amount of every class that reaches the outlet,

$$g(\chi_i) \propto w_i\,(\theta_m + \theta_{im}\,r_{im})\,C_i(L)\,, \quad r_{im} = \omega/(\omega + \theta_{im}\,\chi_i)\,, \tag{6}$$

where w_i is the fraction of material entering in class i, r_{im} is the share of that class held in the mobile pore, and the whole is rescaled to unit area. To keep the test fair, we avoid a circular setup, one in which a gamma-shaped reference would be rebuilt with a gamma fit and would win automatically. So we use two different inlet shapes for the weights w_i: a gamma with shape 1.3 and mean 6, and a log-normal with a coefficient of variation of 0.8 (the standard deviation divided by the mean) and mean 6. Boudreau and Ruddick (1991) showed that a gamma-shaped distribution stays gamma-shaped under decay, so the gamma-seeded case already favors the gamma fit; the log-normal seed removes that built-in advantage. A check for negative, unphysical concentrations never triggered in any reactivity case.

2.2.2. The age distribution

For age, we follow a non-reacting tracer by tracking 12000 particles through the same two-pore column, with a time step $\Delta t = 1.5 \times 10^{-3}$. In one step, a particle in the mobile pore moves forward with the flow and takes a small random jump,

$$x_{n+1} = x_n + v\,\Delta t + \sqrt{(2\,D\,\Delta t)}\,\xi_n\,, \quad \xi_n \sim N(0,1)\,, \tag{7}$$

where x_n is the particle position and ξ_n is a random number from a standard normal distribution. During a step, a mobile particle drops into the stagnant pore with probability $(\omega/\theta_m)\,\Delta t$, and a stagnant particle returns to the mobile pore with probability $(\omega/\theta_{im})\,\Delta t$. Every particle still inside the column ages by Δt each step, and its residence time is the age at which it first reaches the outlet at $x = L$. We keep extending the run and the reporting grid, which has 700 points, until fewer than 0.1% of the particles are still inside the column. The reference then captures the whole distribution, tail included. We turn the exit ages into a smooth curve (a kernel density estimate), and we average every age result over five random-number seeds, reporting the scatter between seeds as a standard deviation.

2.3. The five ways we rebuild a distribution

We compare five methods. Each one turns a set of moments into a full density, and all are drawn on the same axis so their errors can be compared. The first two use two parameters, fitted to the mean and the variance. The gamma fit is

$$g\_\Gamma(\chi) = \chi^{a-1}\,e^{-\chi/b} / (b^a\,\Gamma(a))\,, \quad a = \mu^2/\varphi_2\,, \quad b = \varphi_2/\mu\,, \tag{8}$$

and the log-normal fit is

$$g_{LN}(\chi) = 1/(\chi\,\sigma\,\sqrt{(2\pi)})\,\exp(-(\ln\chi - m)^2 / (2\sigma^2))\,, \quad \sigma^2 = \ln(1 + \varphi_2/\mu^2)\,, \quad m = \ln\mu - \sigma^2/2\,. \tag{9}$$

The third method is a translated Weibull, a Weibull shifted along the axis so it can start away from zero. It has three parameters, so it can also match the skewness,

$$g_W(\chi) = (k/\lambda)\,((\chi - \chi_0)/\lambda)^{k-1}\,\exp(-((\chi - \chi_0)/\lambda)^k)\,, \quad \chi \geq \chi_0\,, \tag{10}$$

where k is the shape, λ the scale, and χ_0 the shift. The skewness of a Weibull depends only on its shape, so we find the shape from the target skewness by solving one equation, $\gamma_1(k) = \varphi_3/\varphi_2^{3/2}$; the scale and shift then follow directly, as $\lambda = [\varphi_2/(\Gamma(1+2/k) - \Gamma(1+1/k)^2)]^{1/2}$ and $\chi_0 = \mu - \lambda\,\Gamma(1+1/k)$. The code checks whether that one-variable solve succeeds, and falls back to the gamma fit if it does not, which never happened for the cases here. The fourth method is the triangle used by Rooze et al. (2023). A triangle can only be so lopsided: its skewness cannot pass $2\sqrt{2}/5 = 0.566$. The distributions here are more skewed than that, above 1.3, so no exact triangle exists. When the target skewness passes the limit, the code returns the most skewed triangle that still matches the mean and variance, which we call saturated. The fifth method assumes no particular shape at all. It is the maximum-entropy density, the smoothest curve that still matches the moments,

$$p(\chi) = \exp(-\Sigma_{k=0}^{M}\,\lambda_k\,\chi^k)\,, \tag{11}$$

where the coefficients λ_k are tuned so the density reproduces the first M moments. We solve it over the whole axis $[0, \chi_{max}]$, rather than cutting it off a fixed distance above the mean, so it is compared with the other methods on exactly the same footing. We leave out the Gram–Charlier expansion (a correction series around a Gaussian), because at these skewness levels it produces small negative probabilities, and removing them destroys the moment match it is supposed to provide.

2.4. How we measure the error

We measure the gap between a rebuilt density $p(\chi)$ and the true reference $g(\chi)$ in three ways. The main one is the total-variation distance, simply half the area between the two curves,

$$TV = \tfrac{1}{2} \int |p(\chi) - g(\chi)|\,d\chi\,, \tag{12}$$

which is 0 for identical curves and 1 for curves that never overlap. We use it as the main measure for two reasons. It stays between 0 and 1, and it does not depend on how far the axis is extended. That makes it a fair yardstick when the distribution widens from one mixing regime to the next. The second measure is the Kolmogorov–Smirnov distance, the largest vertical gap between the two cumulative curves. To show where the gap sits, we split the axis at the 90th percentile of the reference, q90, and form a relative error over the upper tail and over the bulk,

$$E_{tail} = \int_{q90} |p - g|\,d\chi \,/\, \int_{q90} g\,d\chi\,, \quad E_{bulk} = \int_0^{q90} |p - g|\,d\chi \,/\, \int_0^{q90} g\,d\chi\,, \tag{13}$$

so the tail and the bulk are put on the same relative scale. Reporting both avoids a common trap: comparing an absolute error over the whole curve with a relative error in the tail, which can make any error look tail-heavy.

2.5. A precomputed lookup table

The step from a set of scaled moments to a scaled shape is always the same calculation, so we can work out the maximum-entropy fit once, store it, and reuse it. We tabulate it on a grid in the coefficient of variation and the skewness, and read it back by linear interpolation when the model runs. We also record which grid points fail to solve, judged by the leftover moment mismatch at the end of the solve. A failure marks the edge of the region where a valid distribution exists, a curved boundary rather than a simple rectangle in these coordinates. We store the density on the scaled axis χ/μ up to 8, so the tail is kept, and we compare the table with the live solve two ways:

in accuracy, over 300 random test cases, and in speed, against the live maximum-entropy solve and against the gamma and Weibull fits.

The analysis was carried out in R. During preparation the author used a large language model to help draft text, write analysis code, and produce figures; the author checked and verified all content, results, and figures, and takes full responsibility for the work.

3. Results and Discussion

3.1. The matched shape wins, and it is not always the gamma

Figure 1 shows the rebuilt distributions for the two reactivity references and the age distribution, and Table 2 lists the error of every fit on every reference. In every case the fit whose shape matches the true shape wins, and it is not always the gamma. On the gamma-seeded reactivity reference the gamma fit is best, at a total-variation error of 0.018, exactly as expected, since Boudreau and Ruddick (1991) showed that a gamma stays gamma under decay. On the log-normal-seeded reference the log-normal fit is best, at 0.029, and the gamma is worse, at 0.041. On the skewed age distribution the flexible Weibull is best, at 0.059, well ahead of the gamma at 0.145. In every case a matched two- or three-parameter shape reaches an accuracy that the shape-neutral maximum-entropy fit reaches only near four moments, as Fig. 2 shows. Choosing the right shape is therefore worth about one to two extra moments. The triangle cannot capture the skewness of any of these references, and we show it only to make that limit clear.

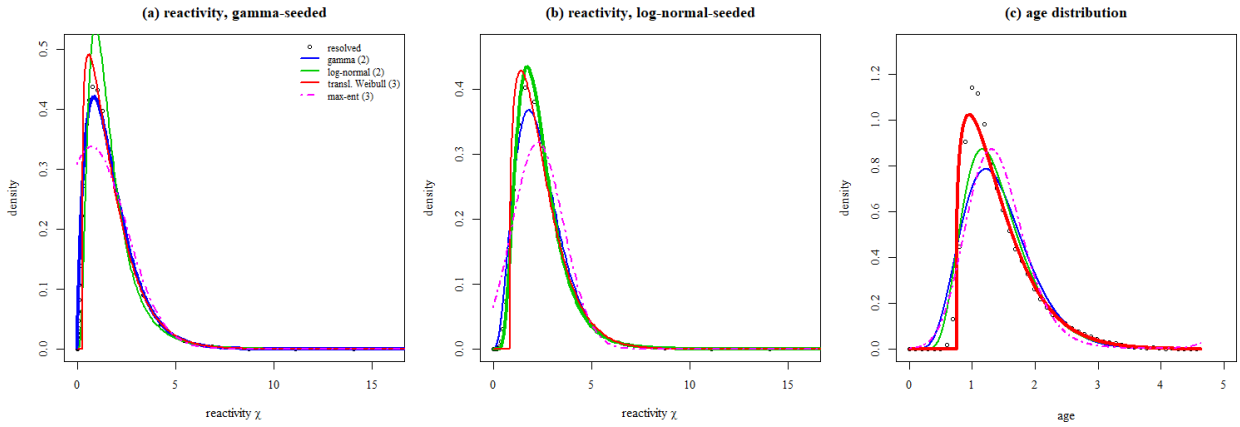

Figure 1. Reconstructions from the moments of the two reactivity references (gamma-seeded and log-normal-seeded) and the age distribution. Open circles show the true resolved reference; the blue, green and red curves are the gamma, log-normal and translated Weibull fits, and the magenta dot-dash curve is the maximum-entropy fit. The thicker curve is the best fit in each panel, and the winner is the shape that matches the reference.

Table 2. Reconstruction error at a mixing time $\tau_m = 0.3$, for the full grid of fits and references. TV is the total variation, KS the Kolmogorov–Smirnov distance, and bulk and tail are the relative errors below and above the 90th percentile. Age values are the mean over five particle-tracking seeds, with the seed-to-seed standard deviation of TV; both reactivity references are complete, with the solver guard inactive for all 600 classes.

Reference	Fit	TV	KS	bulk	tail

Reactivity, gamma	gamma (2)	0.018	0.010	0.03	0.04
(CV 0.71, skew 1.56)	log-normal (2)	0.088	0.056	0.18	0.18
	translated Weibull (3)	0.054	0.035	0.12	0.04
	triangular (saturated)	0.159	0.076	0.28	0.70
	maximum entropy (2)	0.110	0.061	0.21	0.27
	maximum entropy (3)	0.106	0.057	0.21	0.26
	maximum entropy (4)	0.058	0.022	0.11	0.15
Reactivity, log-normal	log-normal (2)	0.029	0.016	0.06	0.07
(CV 0.50, skew 1.33)	gamma (2)	0.041	0.021	0.08	0.10
	translated Weibull (3)	0.064	0.035	0.14	0.07
	triangular (saturated)	0.149	0.064	0.26	0.65
	maximum entropy (2)	0.149	0.067	0.29	0.35
	maximum entropy (3)	0.142	0.065	0.28	0.33
	maximum entropy (4)	0.055	0.024	0.10	0.18
Age (5 seeds)	translated Weibull (3)	0.059 ± 0.002	0.025	0.12	0.06
(CV 0.38, skew ~1.5)	log-normal (2)	0.103 ± 0.004	0.048	0.22	0.11
	gamma (2)	0.145 ± 0.004	0.070	0.30	0.19
	maximum entropy (3)	0.170 ± 0.002	0.082	0.33	0.39
	triangular (saturated)	0.183 ± 0.008	0.096	0.34	0.64

3.2. How many moments, and which shape

Figure 2 shows the maximum-entropy error falling as more moments are supplied, with the two-moment matched shapes drawn as flat reference lines. On the gamma-seeded case the two-moment gamma, at 0.018, is not matched by maximum entropy until four moments, at 0.058. On the log-

normal-seeded case the two-moment log-normal, at 0.029, is likewise reached only near four moments, at 0.055. So a two-moment matched shape beats maximum entropy at three moments. This is a real property of the maximum-entropy form, not a trick of where the axis is cut, because it holds once every fit is on the same axis. The practical message is that a well-chosen shape is worth one to two extra moments for free.

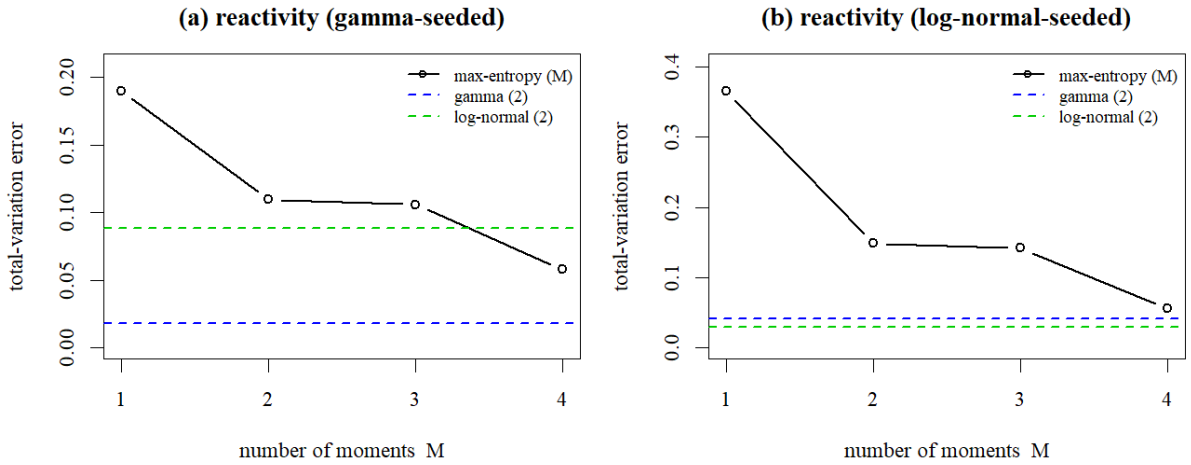

Figure 2. Total-variation error against the number of moments for the maximum-entropy fit (open circles) on the common axis, with the two-moment gamma (blue) and log-normal (green) fits drawn as horizontal reference lines, for the gamma-seeded (a) and log-normal-seeded (b) reactivity references.

3.3. The error grows as mixing increases

Figure 3 sweeps the pore-scale mixing time for the age distribution. We express it as a dimensionless mixing number τ_m / τ_{adv}, where τ_{adv} is the time water needs to cross the column, adjusted for the extra holdup caused by the stagnant pores (retardation),

$$\tau_{adv} = (\theta_m + \theta_{im})\, L / (\theta_m\, v) = 1.43\ . \qquad (14)$$

We report the total-variation error here, which stays between 0 and 1 however wide the distribution becomes, so a rising error cannot simply be a distribution spreading over a wider axis. The error rises steadily with mixing. For the two-moment gamma it climbs from 0.066 to 0.412, for the three-moment Weibull from 0.037 to 0.268, and for three-moment maximum entropy from 0.079 to 0.443, as the mixing number goes from 0.10 to 0.70, with a seed-to-seed scatter of 0.004 to 0.010. The particle reference is complete at every point, with fewer than 0.1% of particles still in the column, so the trend belongs to the reconstruction and is not a reference losing its tail. The tail error rises in the same way. How many moments are needed for a given accuracy therefore depends on the regime, and the matched, skew-aware shape keeps its lead across the whole range.

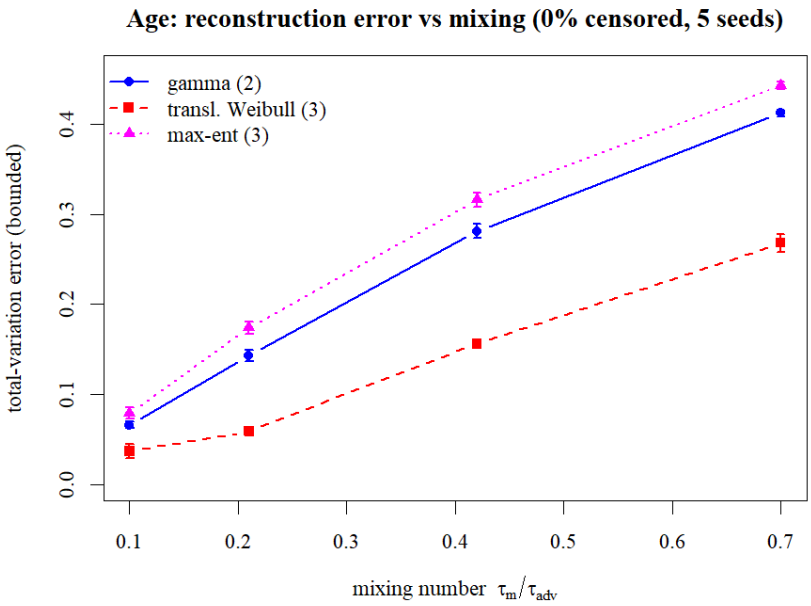

Figure 3. Total-variation reconstruction error for the age distribution against the dimensionless mixing number τ_m / τ_{adv}, for the gamma, translated Weibull and maximum-entropy fits. The total variation stays between 0 and 1 and does not depend on the width of the axis. The particle reference is complete at every point, and the error bars are the seed-to-seed standard deviation over five seeds.

3.4. A precomputed lookup, and when it is worth it

Figure 4 reports the lookup table. Over 300 random test cases inside the tabulated region, it reproduces the live maximum-entropy density to a mean error of 0.001 and a worst case of 0.004, and no grid point in that region failed to solve. In speed, taken as a median over many repeated calls on this reference implementation, the live maximum-entropy solve takes 41 ms and the table takes 0.059 ms, about 700 times faster. The honest catch is that the fits we actually recommend are already cheap without any table: the gamma runs in 0.19 ms and the Weibull in 0.27 ms, one to two orders of magnitude faster than the live maximum-entropy solve. So the table is worth building only when the shape-neutral maximum-entropy fit is really needed; for the recommended simple fits it adds nothing. The absolute times depend on the machine and its load, so the steady number is the ratio, and a maximum-entropy solver built for speed, with a hand-coded derivative and a warm start, would shrink the gap.

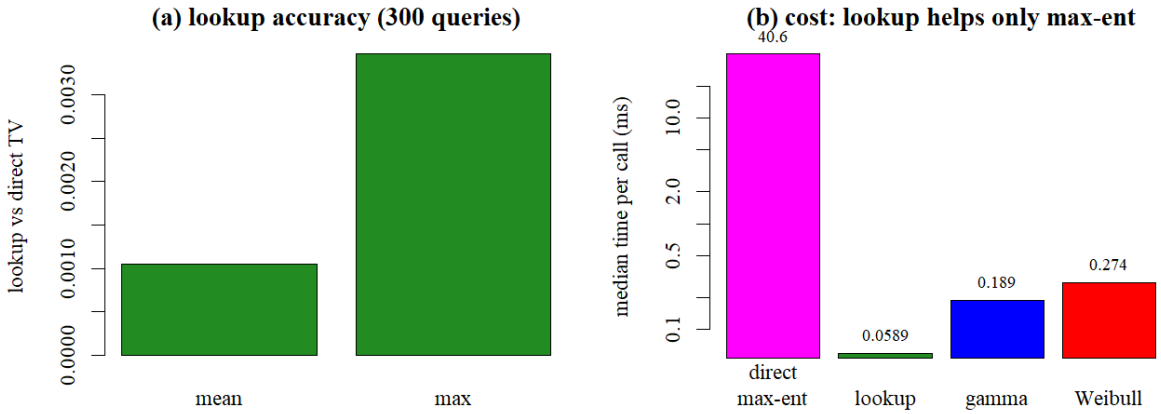

Figure 4. Precomputed lookup table. (a) Accuracy relative to the live maximum-entropy solve over 300 test cases. (b) Median time per call on a logarithmic axis. The table speeds up the maximum-entropy solve, but the recommended gamma and Weibull fits are already far cheaper than that solve, with no table at all.

3.5. From exact to transported moments

The tests so far give each method the exact moments of a known reference, which isolates the reconstruction error on its own. A working model, though, never has exact moments; it carries approximate ones down the domain. To connect the two, we take the strong-flow limit of the reactivity distribution, where mixing is ignored and every parcel moves at the same speed (plug flow), so the outlet distribution is known exactly,

$$g_{out}(\chi) = g_0(\chi)\,\exp(-\chi\, L / v)\,, \tag{15}$$

where $g_0(\chi)$ is the inlet distribution. Both the true outlet and its exact moments are then known, and we widen the axis to $\chi \in [10^{-3}, 80]$ here to hold the longer log-normal tail. We carry the moments down the column with the moment equations, approximate the highest one with a chosen shape, and rebuild the outlet from the carried moments; the guard against a negative carried variance never triggered. For a gamma inlet, whose distribution stays gamma under decay, the gamma fit is exact, so the end-to-end error equals the reconstruction error, which is zero. For a log-normal inlet the fit is only approximate, and the error made while carrying the moments takes over. With a mismatched gamma fit the outlet mean comes out 37% too low and the end-to-end error reaches 0.37, against 0.04 from exact moments. Matching the shape with a log-normal fit halves the mean error to 15% and the total variation to 0.17. Two lessons follow. First, the reconstruction error measured on its own, in Sects. 3.1 to 3.3, is a floor on the end-to-end error, which also carries the moment-transport error, and that transport error can be the larger of the two. Second, the same rule works at both stages, because matching the shape to the truth improves the moment transport as well as the reconstruction.

3.6. What holds up, and the limits

Two findings are solid. First, the reconstruction error is set by how well the assumed shape matches the true shape, and the winning shape follows the truth rather than always being the gamma; the log-normal-seeded case, where the log-normal beats the gamma, removes the circular reasoning a

gamma-only test would carry. Second, the error grows with mixing, and since we measure it with a bounded error and confirm it against a reference whose tail is complete, it belongs to the reconstruction and not to a shrinking tail or a widening axis. It is also worth saying where the error sits. On the same relative scale, the fitted shapes carry a bulk error as large as, or larger than, their tail error; for the age distribution the gamma bulk error of 0.30 is above its tail error of 0.19, and the same order holds for the log-normal and the Weibull. Only the hard-edged saturated triangle, and to a smaller degree the shape-neutral maximum-entropy fit, is strongly tail-heavy. The earlier idea that the error always sits in the tail came from comparing an absolute error over the whole curve with a relative error in the tail.

The study has clear limits. The references are one-dimensional and use a single mixing time, whereas a spread of exchange rates would lengthen the tail. The Péclet number is held fixed at 100 and is not varied, so no result here is a function of it. The maximum-entropy solve is limited to four moments, beyond which it becomes numerically fragile near the edge of the valid region. The end-to-end test of Sect. 3.5 is a strong-flow plug-flow limit with a single fit per inlet; a fuller study would restore mixing, try several fits, and include the exchange between the mobile and immobile pores. Relative to Rooze et al. (2023), who first raised the reconstruction problem, its tail sensitivity, the triangular breakdown, and the lookup idea, the contribution here is a controlled, unbiased, multi-shape comparison with error bars, a corrected axis, clearer sourcing, and a quantified lookup, using the moment-reconstruction methods long established in aerosol and population-balance modeling.

4. Conclusion

Central-moment models are cheap because they carry only a few numbers, but those numbers are useful only if the distribution can be rebuilt from them. Across gamma-seeded and log-normal-seeded reactivity references and a skewed age distribution, the reconstruction error is set by matching the assumed shape to the true shape. The gamma wins when the truth is close to gamma, the log-normal wins when it is log-normal, and the flexible Weibull wins for the skewed age distribution, while the shape-neutral maximum-entropy fit needs about four moments to match a well-chosen two- or three-parameter shape. The error grows with mixing, measured with a bounded error and confirmed against a complete reference, and the triangle cannot be used at all because its skewness is capped at 0.566. Storing the maximum-entropy fit in a lookup table makes it about 700 times faster at a mean error of 0.001, but the recommended simple fits are already cheaper than the maximum-entropy solve, so the table is only for the one case where maximum entropy is needed. Finally, an end-to-end test, in which the moments are carried rather than taken as exact, shows that the reconstruction error measured here is a floor: the moment-transport error can be the larger part, and matching the shape to the truth helps at both stages. In practice, then, pick the shape from the expected shape of the distribution, use three moments and a skew-aware shape when the transport is strongly mixing-limited, and keep the maximum-entropy fit, with its lookup table, for cases where the shape is unknown in advance.

This work is useful wherever a pore-scale or reactive-transport model needs a full distribution of values rather than a single average. Two such distributions run through this paper. The water leaving a sample does not all share one age; it carries a distribution of ages, its residence-time distribution. The organic matter in a sediment does not decay at a single rate; it carries a

distribution of decay rates, a reactivity continuum. Distributions of this kind are common in the field, for example the residence times of water in a streambed or an aquifer, the age of groundwater, and the range of degradation rates in buried organic matter. In each case it is the full distribution, not its mean, that controls the transport or the reaction the model must predict. A central-moment model transports only a few moments cheaply, but the quantity of interest is the distribution itself, which has to be rebuilt from those moments. Our results guide that step: choose the reconstruction shape to match the expected form of the distribution, a gamma or log-normal for a reactivity continuum and a skew-aware Weibull for a residence-time distribution, and expect the largest errors in strongly mixing-limited settings, such as dual-porosity media with large stagnant, immobile pore volumes.

References

Abramov, R.V.: The multidimensional maximum entropy moment problem: a review of numerical methods. Commun. Math. Sci. 8, 377–392 (2010)

Arndt, S., Jorgensen, B.B., LaRowe, D.E., Middelburg, J.J., Pancost, R.D., Regnier, P.: Quantifying the degradation of organic matter in marine sediments. Earth-Sci. Rev. 123, 53–86 (2013). https://doi.org/10.1016/j.earscirev.2013.02.008

Boudreau, B.P., Ruddick, B.R.: On a reactive distribution representation of organic matter diagenesis. Am. J. Sci. 291, 507–538 (1991). https://doi.org/10.2475/ajs.291.5.507

Ginn, T.R.: On the distribution of multicomponent mixtures over generalized exposure time in subsurface flow and reactive transport. Water Resour. Res. 35, 1395–1407 (1999). https://doi.org/10.1029/1999WR900013

John, V., Angelov, I., Öncül, A.A., Thévenin, D.: Techniques for the reconstruction of a distribution from a finite number of its moments. Chem. Eng. Sci. 62, 2890–2904 (2007). https://doi.org/10.1016/j.ces.2007.02.041

Junk, M.: Domain of definition of Levermore-s five-moment system. J. Stat. Phys. 93, 1143–1167 (1998). https://doi.org/10.1023/B:JOSS.0000033155.07331.d9

Levermore, C.D.: Moment closure hierarchies for kinetic theories. J. Stat. Phys. 83, 1021–1065 (1996). https://doi.org/10.1007/BF02179552

Marchisio, D.L., Fox, R.O.: Solution of population balance equations using the direct quadrature method of moments. J. Aerosol Sci. 36, 43–73 (2005). https://doi.org/10.1016/j.jaerosci.2004.07.009

McGraw, R.: Description of aerosol dynamics by the quadrature method of moments. Aerosol Sci. Technol. 27, 255–265 (1997). https://doi.org/10.1080/02786829708965471

Mead, L.R., Papanicolaou, N.: Maximum entropy in the problem of moments. J. Math. Phys. 25, 2404–2417 (1984). https://doi.org/10.1063/1.526446

Rooze, J.: A novel Eulerian model based on central moments (code). Zenodo (2023). https://doi.org/10.5281/zenodo.10202341

Rooze, J., Jung, H., Radtke, H.: A novel Eulerian model based on central moments to simulate age and reactivity distributions interacting with mixing processes. Geosci. Model Dev. 16, 7107–7121 (2023). https://doi.org/10.5194/gmd-16-7107-2023

Yuan, C., Laurent, F., Fox, R.O.: An extended quadrature method of moments for population balance equations. J. Aerosol Sci. 51, 1–23 (2012). https://doi.org/10.1016/j.jaerosci.2012.04.003

Statements and Declarations

Funding The author declares that no specific funding was received for this work.

Competing Interests The author has no relevant financial or non-financial interests to disclose.

Author Contributions Shahram Asgari designed the study, implemented the reconstruction methods and the analysis, produced the figures, and wrote the manuscript.

Use of Generative AI The author used a large language model to edit the manuscript for grammar and readability. The author reviewed and verified all content, results, and figures, and takes full responsibility for the work.

Data and Code Availability All computations are implemented in R, in the single script reconstruction_study_revised.R, which reproduces every number and figure reported here. The script and its generated figures and tables are archived on Zenodo (DOI to be added in the next version). The original central-moment model code that motivated this work is available from Rooze et al. (2023) at https://doi.org/10.5281/zenodo.10202341 (MIT License). No measured data were used.